Shaped Apertures in Photoresist Films Enhance the Lifetime and Mechanical Stability of Suspended Lipid Bilayers

Sumit Kalsi,[†‡*] Andrew M. Powl,[§] B. A. Wallace,[§] Hywel Morgan,[†‡] and Maurits R. R. de Planque[†‡*]
[†]Electronics and Computer Science and [‡]Institute for Life Sciences, University of Southampton, Southampton, United Kingdom; and [§]Institute of Structural and Molecular Biology, Birkbeck College, University of London, London, United Kingdom

ABSTRACT Planar lipid bilayers suspended in apertures provide a controlled environment for ion channel studies. However, short lifetimes and poor mechanical stability of suspended bilayers limit the experimental throughput of bilayer electrophysiology experiments. Although bilayers are more stable in smaller apertures, ion channel incorporation through vesicle fusion with the suspended bilayer becomes increasingly difficult. In an alternative bilayer stabilization approach, we have developed shaped apertures in SU8 photoresist that have tapered sidewalls and a minimum diameter between 60 and 100 μm. Bilayers formed at the thin tip of these shaped apertures, either with the painting or the folding method, display drastically increased lifetimes, typically >20 h, and mechanical stability, being able to withstand extensive perturbation of the buffer solution. Single-channel electrical recordings of the peptide alamethicin and of the proteoliposome-delivered potassium channel KcsA demonstrate channel conductance with low noise, made possible by the small capacitance of the 50 μm thick SU8 septum, which is only thinned around the aperture, and unimpeded proteoliposome fusion, enabled by the large aperture diameter. We anticipate that these shaped apertures with micrometer edge thickness can substantially enhance the throughput of channel characterization by bilayer lipid membrane electrophysiology, especially in combination with automated parallel bilayer platforms.

INTRODUCTION

Electrical measurements of ion permeation are the most powerful methods to characterize ion channel function, especially at the single-channel level, and its modulation by agonists and antagonists, including pharmacological drugs (1,2). Of the two main electrophysiology variations, patch clamping of natural cell membranes relies on cellular expression and membrane incorporation of the channel of interest, at a low background of endogenous channels (3,4), whereas bilayer lipid membrane (BLM) electrophysiology typically involves incorporation, by proteoliposome fusion, of a purified ion channel into a planar bilayer of synthetic phospholipids (5–8). Although the BLM method has some distinct advantages, most notably the possibility to obtain the channel from any desired expression system and control over the lipid composition of a bilayer that does not contain any other ion channels, it suffers from low throughput due to the fragility of the planar bilayers.

In a conventional BLM experiment, the lipid bilayer is suspended in an aperture with a diameter of ~100–200 μm in a thin septum that separates two aqueous chambers, each of which accommodates an electrode connected to an amplifier. The aperture-suspended bilayer is formed by the Mueller-Rudin (painting) method, in which an oil-lipid solution is deposited on the aperture and the bilayer forms when the oil phase has thinned to a sufficient extent (9), or by the Montal-Mueller (folding) method (10), in which an air-water interface with a lipid monolayer is raised over both sides of the aperture, which is typically pretreated with an apolar solvent (11,12). Although the folding method involves a substantially smaller amount of solvent than the painting method, both protocols result in a planar bilayer that is connected to the wall of the aperture by a solvent annulus, which is also referred to as the Plateau Gibbs border (6,12–15). The septum material should be sufficiently hydrophobic to enable draining of excess solvent, have suitable electrical properties (high resistivity, low dielectric constant, and low dielectric loss), be mechanically strong, and chemically compatible with cleaning solutions (16,17).

Widely used septa are Teflon films of 10–50 μm thickness and locally thinned walls of monolithic polystyrene cuvettes (6,17,18). Apertures in these polymers are created by relatively coarse methods such as mechanical punching, microdrilling, or electrical spark ablation (17–19), which do not give fine control over the aperture diameter and geometry, and hence the ease of bilayer formation and the bilayer stability varies considerably between apertures. Even under optimal conditions (i.e., with good apertures), the lifetime of the suspended bilayer is <3 h (5,20–22), and in our experience, minimal perturbation of the aqueous chambers tends to cause bilayer failure. To improve bilayer stability, several groups have used lithographic techniques to reproducibly fabricate apertures of a well-defined size and circularity in glass, silicon, or surface-modified photopolymers (23–29).

Photolithography has also enabled the fabrication of apertures that are substantially smaller, down to hundreds of nanometers, than conventional micromachined apertures.

Submitted October 21, 2013, and accepted for publication February 26, 2014.

*Correspondence: sk24g09@ecs.soton.ac.uk or mdp@ecs.soton.ac.uk

Editor: Claudia Steinem.

0006-3495/14/04/1650/10 $2.00

http://dx.doi.org/10.1016/j.bpj.2014.02.033

It is well known that smaller apertures improve the stability of suspended bilayers (17–19,30–37). For example, a POPC bilayer lifetime of 75 h has been reported for 200 nm apertures in silicon nitride, but without using an ion channel (32). But since fabrication-focused studies tend to verify bilayer suitability for ion channel incorporation with water-soluble ion channels, it is often overlooked that submicron or few-micron bilayers apertures (~<30 μm) are not suitable for proteoliposome fusion with the suspended bilayer (6,38,39). A reduction in aperture diameter also necessitates a reduction in septum thickness to avoid unstirred layer effects near the bilayer surface and a high convergence resistance at the opening of high aspect ratio apertures (16,40). Moreover, based on an analysis of bilayer/annulus and annulus/septum contact angles, it has been predicted that large-area stable suspended bilayers can be formed when a very thin septum is used (14).

Hence, reducing the aperture diameter to some extent while thinning the septum as much as possible, appears to be the most promising strategy to obtain stable bilayers that are sufficiently large to facilitate proteoliposome fusion. But thin septa (<20 μm) are less mechanically robust, and more importantly, increase the septum capacitance and therefore contribute more noise to the electrical recording, which limits the measurement bandwidth (16,17). However, the problems of mechanical instability and high septum capacitance can be avoided by only thinning the septum locally, or in other words, by realizing a geometry with a thin aperture wall that tapers out to the full thickness of the bulk septum. Such tapered apertures can be obtained by mechanical punching with a conical tip (17), but reproducible fabrication of shaped apertures requires lithography methods, which have been explored in a small number of studies. Triangle-shaped apertures with inner diameters ranging from 10 to 60 μm have been fabricated in silicon nitride and in the resists polyimide and SU8, and were shown to support ion channel activity of gramicidin and alamethicin and of proteoliposome-delivered hERG channel and nicotinic acetylcholine receptor in painted bilayers of phosphatidylcholine or folded bilayers of phosphatidylcholine/phosphatidylethanolamine/cholesterol, which were stable for tens of hours (41–47).

Here, we present a set of tapered apertures with different shapes and with different diameters, fabricated in the photoresist SU8 by two-photon stereolithography. The stability of bilayers suspended in these apertures was systematically evaluated by establishing the number of times the buffer-air interface could be moved over the aperture until the bilayer failed. The experiments clearly demonstrate that tapered apertures give bilayers that are substantially more stable than nontapered apertures, both in terms of bilayer lifetime and of mechanical stability. The bilayer lifetime is reduced when the narrowest part of a beak-shaped aperture is thickened from ~2 to ~10 μm, and also when the diameter is increased from 60 to 100 μm, confirming the stability criteria outlined previously. We tested these apertures with two different types of channels, the polypeptide alamethicin, which could be added in organic solvent to form well-characterized multilevel channels (25), and the KcsA potassium channel, a macromolecular tetrameric channel (48), which was added in proteoliposomes. As the small diameter apertures did not consistently result in KcsA channel activity, our final design consisted of a 80 μm (designed) diameter beak-shaped aperture, in which bilayers were stable for typically >20 h. Because the SU8 septum is 50 μm thick, enabling mounting in conventional bilayer chambers without support materials, and with a capacitance of just 18 pF is suitable for high-bandwidth recordings, we anticipate that these shaped apertures can substantially enhance the throughput of BLM electrophysiology experiments, especially in combination with multibilayer automated systems.

MATERIALS AND METHODS

Fabrication of SU8 apertures

A 30 mm diameter glass substrate (Menzel-Gläser, Braunschweig, Germany) was acid cleaned and dried overnight at 210°C. A sacrificial layer of LOR 7B resist (MicroChem, Newton, MA) was spin-coated on the substrate at 1500 rpm for 60 s and soft baked at 150°C for 3 min. After allowing the substrate to cool for 15 min, SU8 3050 resist (MicroChem) was spin-coated at 3000 rpm for 30 s and soft baked at 95°C for 15 min to obtain a thickness of ~50 μm. A coordinate file for a shaped aperture was created with SolidWorks (Dassault Systèmes, SolidWorks Corp., Vèlizy, France) and exported to a Photonic Professional laser lithography system (Nanoscribe, Eggenstein-Leopoldshafen Germany), which exposed the SU8 film at the desired positions within a 400 × 400 μm area. The substrate was then baked for 90 s at 65°C to stabilize the cross-linked SU8. The part of the SU8 film outside this area was now exposed, through a mask that protected the laser lithography defined area, at 250 mJ/cm^2 in a conventional mask aligner, giving a polymerized SU8 sheet of 2 × 2 cm with the aperture at the center position. The substrate was postbaked first at 65°C for 1 min and then at 95°C for 4 min, and the nonpolymerized SU8 regions were removed by development in EC solvent (MicroChem) for 5 min. The SU8 layer was subsequently released from the glass substrate by dipping in AZ 726 MIF developer (AZ Electronic Materials, Luxembourg), which solubilized the LOR 7B sacrificial layer. The released SU8 layer was subsequently dip-coated with the fluoropolymer CYTOP (AGC Chemicals, Thornton Cleveleys, UK) or was vapor coated with Parylene C (poly-(para-xylylene)) using a Labcoater 2 Parylene Deposition System (Specialty Coating Systems, Indianapolis, IN). Scanning electron microscopy (SEM) and optical microscopy were performed with EVO LS25 and LSM 5 Exciter microscopes (Carl Zeiss, Jena, Germany).

Lipid bilayer formation

The phospholipids, 1,2-dioleoyl-*sn*-glycero-3-phosphocholine (DOPC), 1-palmitoyl-2-oleoyl-*sn*-glycero-3-phospho-(1′-rac-glycerol) (POPG), 1,2-diphytanoyl-*sn*-glycero-3-phosphocholine (DPhPC), and 1,2-dioleoyl-*sn*-glycero-3-phosphoethanolamine-*N*-(lissamine rhodamine B sulfonyl) (fluo-DOPE) were purchased from Avanti Polar Lipids (Alabaster, AL). The SU8 sheet with the lithography defined shaped aperture was clamped between two Teflon chambers of 1.25 ml volume such that the SU8 septum was in contact (5 × 7 mm area) with the aqueous phase of both chambers.

Aperture-suspended bilayers were prepared with the painting or the folding method. For the painting method, lipids were dissolved in decane or nonane at a total lipid concentration of 20 mg/ml by solvent solubilization of a mixed lipid film, obtained by mixing and drying of lipid stock solutions in chloroform. The lipid-solvent solution was painted on the aperture with a Sable 0000 paint brush, and the buffer-air interface of the buffer solution in each compartment was raised and lowered over the aperture to promote solvent draining and bilayer formation (49). For the folding method, the aperture was pretreated with 5% hexadecane in hexane. Lipids in volatile solvent, chloroform or hexane, (~7–10 μl of a 20 mg/ml solution) were placed on top of the buffer solution in each compartment and the solvent was allowed to evaporate. The buffer-air interface was then raised and lowered over the aperture until a bilayer was formed by monolayer opposition. For optically accessible bilayers, the SU8 sheet was clamped in a homemade microfluidic chip of poly(methyl methacrylate) (PMMA), giving a distance from the aperture to the surface of the glass coverslip of ~300 μm. The PMMA chip was mounted onto a Zeiss Axiovert 200 (Carl Zeiss) inverted fluorescence microscope for optical imaging of the painted horizontal bilayer.

KcsA ion channel reconstitution

The potassium channel KcsA was expressed and purified according to previously published procedures (48). Reconstitution into lipid vesicles was performed by detergent depletion. Bio-beads SM-2 (Biorad Laboratories, Hemel Hempstead, UK) were cleaned in methanol for 30 min followed by thorough rinsing with electrophysiology buffer (150 mM KCl, 10 mM HEPES, pH 7.4). Phospholipid solutions in chloroform were mixed in the desired combination (3 μmol total lipid) and dried onto the walls of a glass vial as a mixed lipid film. The lipid film was subsequently dissolved in 1 ml of reconstitution buffer (40 mM β-D-octyl glucoside, 150 mM KCl, 10 mM HEPES, pH 7.4), with bath sonication to clarity for at least 30 min. KcsA in detergent solution (1.9 mg/ml in dodecyl β-D-maltoside (Sigma Aldrich, St. Louis, MO) (60 μg protein) was added to achieve a 3333:1 molar ratio of lipid/KcsA tetramer. The β-D-octyl glucoside detergent (Sigma Aldrich) was gradually removed by an initial one-hour incubation with 80 mg of washed Bio-beads, followed by a second one-hour incubation with 80 mg of fresh Bio-beads. The proteoliposomes were then removed from the Bio-beads and stored at +4°C until use. The diameter of the proteoliposomes as determined by dynamic light scattering (Zetasizer Nano ZS, Malvern Instruments, Malvern, UK) was ~125 nm.

Single-channel measurements

Ag/AgCl wire electrodes were placed into the two aqueous compartments of the Teflon bilayer cell and were connected to a high sensitivity ID562 BLM amplifier (Industrial Developments Bangor, Bangor, UK). Bilayer formation was monitored by capacitance measurements. A linear voltage ramp of $\pm$1 V/s (50 mV peak-to-peak triangle waveform, 500 Hz frequency) was applied, the current signal was displayed on a digital oscilloscope, with a square current waveform indicating bilayer formation, and the value of the capacitance was derived from the current amplitude of this waveform. After successful formation of a lipid bilayer, a DC potential of |100–200 mV| was applied to measure the bilayer current. The current signal was digitized at 5 kHz with a homebuilt LabVIEW (National Instruments, Austin, TX) user interface. Bilayer traces were analyzed and digitally filtered using a 1 kHz Gaussian filter with Clampfit 10.2 software (Molecular Devices, Sunnyvale, CA). The peptide alamethicin (Sigma Aldrich) was introduced into ethanol in both of the aqueous chambers, each of which contained a solution of 2 M KCl, 10 mM HEPES, pH 7.4, giving an alamethicin concentration in the bilayer chamber of 10 ng/ml. KcsA was introduced as several microliters of proteoliposome suspension, with one compartment containing electrophysiology buffer (150 mM KCl, 10 mM HEPES, pH 7.4) and the other compartment a buffer solution of pH 4.0 (150 mM KCl, 10 mM HEPES, pH 4.0).

Bilayer stability tests

Bilayer formation was adjudged by empirically determined capacitance. All stability tests in SU8 apertures have been carried out on bilayers having capacitance values within 1–1.5$\times$ as expected from the area of the aperture (assuming 0.5–0.7 μF/cm^2). Leaky bilayers and unstable bilayers with a sealing resistance less than a few tens of GΩ were rejected. During bilayer lifetime tests, the aqueous solutions in the bilayer chamber were not perturbed. The tests for evaluating bilayer mechanical stability involved raising and lowering the buffer-air interface over the aperture in either compartment. After addition of ion channels to the compartment, the bilayer was kept at DC voltage >|100 mV|. SU8 sheets were also reused by cleaning the debris inside the aperture at low power agitation in an ultrasonic bath sonicator. If the aperture showed signs of wear around its circumference, the sheet was discarded.

RESULTS

Characterization of shaped apertures in SU8

SU8 is an ultraviolet-curable polymer with a dielectric constant only ~1.5$\times$ that of Teflon which, combined with its excellent chemical and mechanical properties (43), renders it a suitable septum material for low-noise bilayer recordings. Using three-dimensional laser lithography, we fabricated beak-shaped, triangle-shaped, blunted-beak, blocked-beak, and cylindrical apertures, as schematically depicted in Fig. 1. Fig. 2 *A* shows a SEM image of a beak-shaped aperture in a 400 $\times$ 400 μm layer of SU8. All the SU8 in this image has been polymerized by laser stereolithography and nonpolymerized SU8 was washed away with the development solution. To obtain larger, 2 $\times$ 2 cm, sheets of SU8, the area surrounding the laser-defined area was polymerized, before development, by conventional flood exposure, as outlined in the Methods. Fig. 2 *B* shows a top view of a beak-shaped aperture in a SU8 sheet, as well as cross sections, as visualized by confocal laser scanning microscopy with 405 nm excitation, which exploits the absorbance properties of SU8 at a lower wavelength (50,51). SEM and confocal microscopy confirm the fabrication of sloped aperture walls.

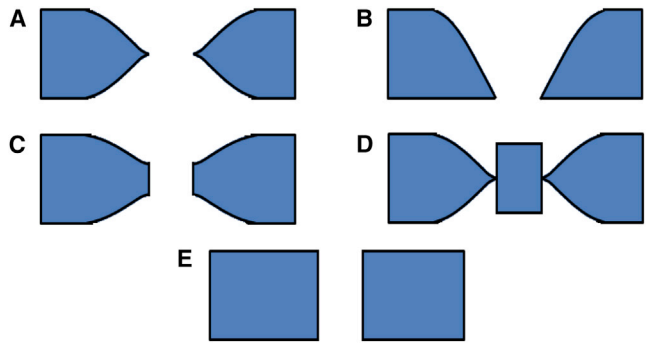

FIGURE 1 Schematic cross-sectional view of the various fabricated apertures: (*A*) beak-shaped, (*B*) triangle-shaped, (*C*) blunted-beak, (*D*) blocked-beak control, and (*E*) cylindrical control. To see this figure in color, go online.

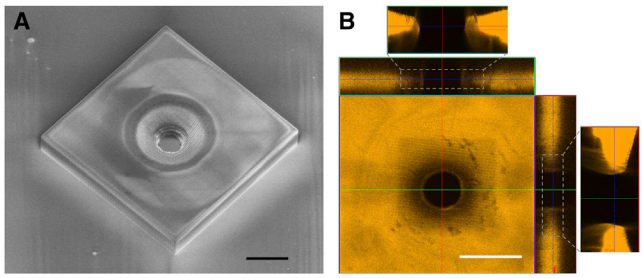

FIGURE 2 (*A*) Beak-shaped aperture written using laser stereolithography in SU8. The remaining unpolymerized resist on the glass substrate has been removed during the development step. (*B*) Confocal laser scanning microscopy of a beak-shaped aperture in a 2 × 2 cm sheet of SU8. The scale bars are 100 μm. To see this figure in color, go online.

Top view and cross-section SEM images of different apertures, before the release of the SU8 sheet from the glass substrate, are shown in Fig. 3. Cylindrical, triangle-shaped, and beak-shaped apertures were fabricated successfully, with observed aperture wall profiles closely matching the designed geometries. At its narrowest point, the triangle-shaped and the beak-shaped apertures have an aperture tip thickness of ~2 μm. A blunted variation of a beak-shaped aperture, with 10 μm thickness was also fabricated (data not shown). The intended values of the diameters of the apertures were 60, 80, or 100 μm for the cylindrical aperture, and 60 or 80 μm for the narrowest points of the triangle-shaped apertures, 60, 80, or 100 μm for the beak-shaped apertures, and 60 μm for the blunted-beak variation. The measured diameters were ~10% larger than the design values (Fig. 3), which may indicate some overdevelopment. Because the SolidWorks design for the shaped aperture contained a tip thickness of a few hundred nanometers, the inner diameter of the aperture in SU8 after the fabrication process was on average ~10% more than the desired dimension due to the washing away of the apex of the tip during SU8 development. The tip thickness could have been reduced below 2 μm, but this would have posed fabrication challenges

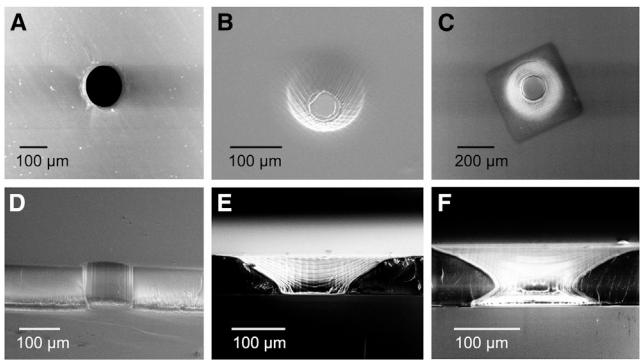

FIGURE 3 Top view (*A–C*) and cross-section view (*D–F*) SEM images of apertures in SU8 sheets that are still attached to the glass substrate: (*A* and *D*) cylindrical, (*B* and *E*) triangular, and (*C* and *F*) beak-shaped.

(damage to the tip) and practical problems associated with cleaning of the aperture, ultimately restricting overall reusability and reproducibility.

The blocked-beak aperture structure was fabricated to enable measurement of the capacitance of the SU8 sheet with the shaped aperture. A value of 18 pF was obtained, which is identical, within the accuracy of the measurement, to the capacitance of a clamped 50-μm thick SU8 sheet without an aperture. This indicates that the rather small area of the sheet that contains thin (<50 μm thickness) SU8 does not significantly increase the capacitance of the septum, which validates the implementation of a shaped aperture rather than using a cylindrical aperture in a thin (~2 μm thickness) sheet of SU8. For comparison, the capacitance of a 50-μm thick sheet of Teflon was measured as 12 pF, reflecting the somewhat smaller dielectric constant of this material.

The fabricated SU8 sheets were tolerant to solvents such as isopropanol and ethanol, which are routinely used for removing lipids, peptides, or proteins from used apertures. Although SU8 is reasonably hydrophobic and has a contact angle of ~70°, initial experiments with painting lipid bilayers in these apertures posed difficulty with thinning the oil-lipid mixture into a lipid bilayer or did not yield continuous ion channel activity. Hence, to improve oil wettability, a thin hydrophobic coating of CYTOP was applied, which increased the contact angle to ~100°. This coating was later replaced with vapor deposited Parylene C (<500 nm), which is more durable and results in a more uniform conformal layer. Septa coated with CYTOP or Parylene C displayed the same bilayer formation and bilayer stability characteristics.

Lipid bilayers in shaped apertures

We used both the Mueller-Rudin painting method (9) and the Montal-Mueller folding method (10) for the formation of aperture-suspended lipid bilayers. The total capacitance was measured and the known septum background capacitance of 18 pF was subtracted to obtain the capacitance of the suspended bilayer. As an example, the total capacitance for folded DOPC/POPG bilayers in an 80 μm diameter beak-shaped aperture was ~50 pF in eight independent experiments (Fig. 4 *A*). Based on a specific bilayer capacitance of 0.7 μF/cm^2 (32,12) the area of the bilayer was estimated and compared with the area of the narrowest part of the aperture, as determined by microscopy. It was found that for various shaped apertures, the folding method resulted in bilayers that consistently occupied ~85% of the available aperture area. On the other hand, the painting method resulted in a range of bilayer areas, most likely due to varying sizes of the oil annulus, which is possibly related to the exact amount of oil-lipid solution applied to the aperture. Moreover, unlike the folded bilayers, the capacitance of the painted bilayers showed a dependence on the applied

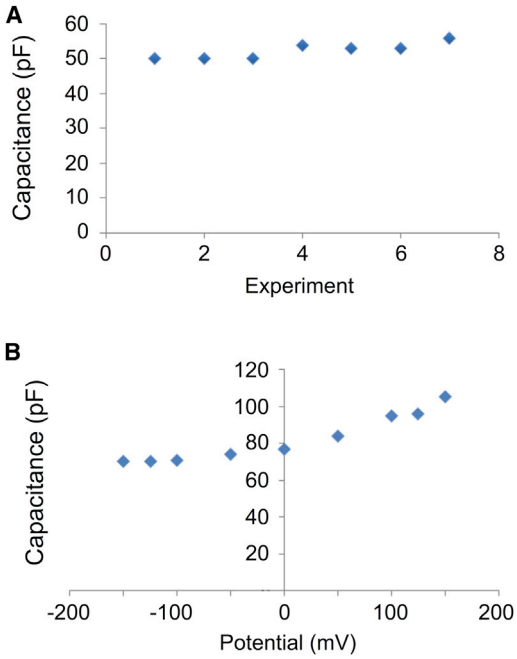

FIGURE 4 (*A*) Capacitance of different DOPC/POPG (1:1 molar ratio) bilayers formed with the folding method using a 20 mg/ml chloroform-lipid solution in an 80 μm diameter beak-shaped aperture. (*B*) Dependence of capacitance on voltage for a DOPC/POPG bilayer (1:1 molar ratio) painted with 20 mg/ml lipid-decane solution in a 100 μm diameter beak-shaped aperture. The background capacitance is 18 pF. To see this figure in color, go online.

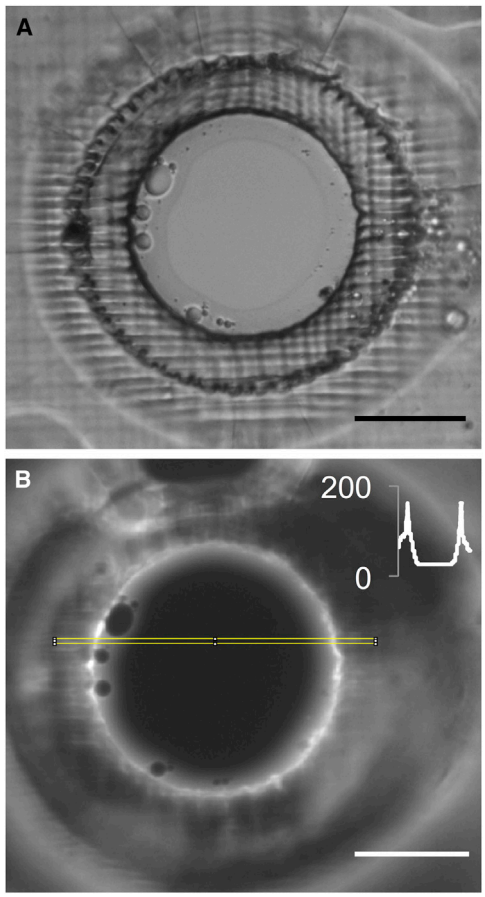

FIGURE 5 (*A*) Bright field and (*B*) fluorescence image of a suspended bilayer in a beak-shaped aperture painted with a DPhPC/fluo-DOPE/decane mixture. The inset shows the fluorescent intensity profile along the yellow line. The scale bars are 50 μm. To see this figure in color, go online.

potential (Fig. 4 *B*), as previously observed by other groups (6,12). However, all the bilayers suspended in beak-shaped and triangle-shaped apertures could easily tolerate potentials up to 200 mV for 1–2 h.

To determine the position of the suspended lipid bilayer in a shaped aperture, bilayers were painted on horizontally positioned SU8 apertures, using a PMMA chip with a 170 μm glass coverslip as the bottom layer, rather than the Teflon chambers that clamp SU8 septa in a vertical orientation. Fig. 5, *A* and *B*, show bright field and fluorescence images of the painted bilayer. The bright field image shows the interface between the bilayer and the decane annulus as a transition from a lighter to a darker region. Because the lipid-oil mixture also contained a fraction of fluorescent lipids, the decane annulus is clearly visible in the fluorescent microscopy image. The slope of the fluorescence intensity profile (Fig. 5 *B*, *inset*) reflects the gradient in thickness of the annulus, with thicker regions containing more fluorescent lipid. Based on the diameter of the decane-lipid annulus and the colocalization of the focal planes of the edge (tip) of the aperture and the bilayer-annulus interface, we conclude that the bilayer has formed at the narrowest part of the aperture. Infrequently, it was observed that bilayers gave a capacitance around 2–3 times greater than an empirically estimated value, which could be due to the formation of the bilayer on the slope of the tapered edge or at the point where the edge starts to taper or due to formation of a cupola-shaped bilayer (52). Such bilayers were not stable and were broken on purpose by agitating the buffer in the chamber via aspiration.

Lifetime of suspended bilayers

To demonstrate the functionality of the lipid bilayers, the water-soluble peptaibol alamethicin from *Trichoderma viride* was added to the aqueous compartments. We selected this multimeric peptide ion channel because of its characteristic voltage dependent conductance (channel gating at $>|60$ mV$|$) and existence of multiple nonequidistant single-channel conductance levels (25). Suspended lipid bilayers should support alamethicin ion channel activity throughout their lifetime.

Bilayers were painted with decane or nonane to obtain suspended lipid bilayers with different molar ratios of DOPC and POPG lipids (see Table 1). As a reference, we first evaluated bilayer stability in the cylindrical SU8 aperture with a diameter of 60 μm. These bilayers were stable

TABLE 1 Lifetime of painted suspended bilayers, for individual experiments, in shaped apertures

Lipid composition	Solvent	Aperture shape/diameter	Lifetime (hours)
3:1 DOPC/POPG	Decane	Cylindrical (60 μm)	2
3:1 DOPC/POPG	Decane	Cylindrical (60 μm)	2
3:1 DOPC/POPG	Decane	Triangle (60 μm)	36
1:1 DOPC/POPG	Decane	Beak (60 μm)	30
1:1 DOPC/POPG	Decane	Beak (60 μm)	21
1:1 DOPC/POPG	Decane	Triangle (60 μm)	31
3:1 DOPC/POPG	Nonane	Beak (80 μm)	30
1:1 DOPC/POPG	Decane	Beak (80 μm)	30

for up to 2 h and disintegrated at potentials $>|150$ mV$|$ ($n = 8$), which is similar to bilayers suspended in a conventional aperture in a Teflon septum (53,54). In marked contrast, painted bilayers in the beak-shaped and triangle-shaped apertures with a tip thickness of ~2 μm were stable for >20 h ($n = 6$) at applied potentials of $>|100$ mV$|$, continuously showing alamethicin channel activity (Fig. 6 *A*). The bilayer lifetime was reduced in the blunted-beak aperture (~10 μm tip thickness) to ~14 h.

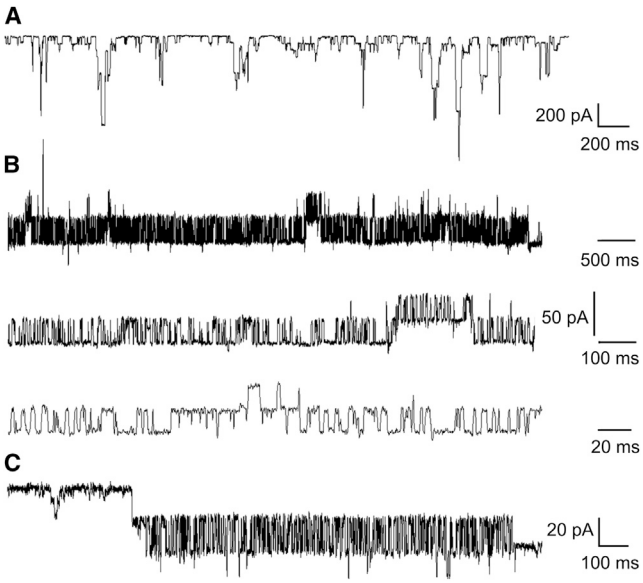

FIGURE 6 (*A*) Alamethicin channel activity, 26 h after bilayer formation, in a DOPC/POPG (1:1 molar ratio) suspended bilayer painted from a lipid-decane solution. The applied potential is −125 mV and the buffer solution is 2 M KCl, 10 mM HEPES, pH 7.4. The aperture is beak-shaped with an inner diameter of 80 μm. (*B*) KcsA ion channel activity in a POPG bilayer painted with a decane-POPG solution on a beak-shaped aperture with an inner diameter of 60 μm (150 mV potential, 150 mM KCl, pH 4.0 in one compartment and pH 7.4 in the second compartment), also shown are zoomed views of the same bilayer trace, depicting individual gating events. (*C*) KcsA ion channel activity in a DOPC/POPG (1:1 molar ratio) bilayer painted with a decane-lipid solution on a beak-shaped aperture with an inner diameter of 80 μm (150 mV potential, 150 mM KCl, pH 4.0 in one compartment and pH 7.4 in the second compartment). The traces in panel *B* and *C* are representative bursts of KcsA activity, selected from 10 independent experiments.

These experiments highlight the relationship between aperture edge thickness and bilayer stability.

Although bilayer stability in the 80 μm beak-shaped aperture was the same when nonane or decane was used as the painting oil (Table 1), decane was preferred because of its reduced tendency to partition into the lipid bilayer (55). The diameter of the narrowest part of the beak-shaped aperture was 60, 80, or 100 μm, keeping the diameter of the widest part of the aperture (i.e., at the septum surface) constant at 250 μm. There was no apparent difference in bilayer stability in the 60 and 80 μm diameter apertures (Table 1) but for the 100 μm diameter aperture, the painted bilayer lifetime was reduced to only a few hours (data not shown). We speculate that, as the 100 μm aperture geometry more closely resembles a cylindrical aperture, the oil annulus gradually drains away, eventually causing bilayer failure (14).

Next, we evaluated the lifetime of folded bilayers, which were found to be stable for ~20 h in triangle-shaped and beak-shaped apertures (Table 2). It was observed that folded bilayers were easier to form in beak-shaped apertures than in triangle-shaped apertures, which may relate to the mechanism of the folding method, where a lipid-air monolayer is brought into contact with each side of the aperture separately. We speculate that the tapered side of a triangle-shaped aperture facilitates the formation of a suspended bilayer, whereas the flat side of the aperture does not.

Mechanical stability of lipid bilayers

Perturbation of the aqueous solution in contact with a lipid bilayer is required to mix a small volume of an added concentrated solution, for example a channel blocker, with the electrophysiology buffer, or to change the buffer solution by successive removal of a fixed volume of the original buffer and addition of the same volume of the new buffer. In the case of ion channel incorporation by proteoliposome fusion, it has also been observed that moving the buffer-air interface over the aperture promotes liposome fusion with the suspended bilayer (56,57). For this reason, we also investigated the mechanical stability of the suspended bilayers by counting the number of times that the buffer-air

TABLE 2 Lifetime of folded suspended bilayers, for individual experiments, in shaped apertures

Lipid composition	Aperture shape/diameter	Lifetime (hours)
DPhPC	Triangle (60 μm)	26
1:1 DOPC/POPG	Cylindrical (80 μm)	≤ 2
1:1 DOPC/POPG	Triangle (80 μm)	15
1:1 DOPC/POPG	Beak (80 μm)	21
1:1 DOPC/POPG	Beak (80 μm)	19
cis DOPC, *trans* POPG	Beak (80 μm)	21

The lifetime for the cylindrical aperture is an estimate based on a large number of bilayer formation experiments.

interface could be moved over the bilayer without causing bilayer failure. This procedure was performed by the gentle aspiration of buffer solution from the bottom of an aqueous compartment into a pipette, and then reintroducing the same volume into the compartment.

Because painted bilayers have a tendency to change their area, as monitored by capacitance measurements, during such aspiration cycles (data not shown), we concentrated on folded bilayers. As depicted in Fig. 7, in 19 bilayer formation experiments with DOPC/POPG bilayers suspended in the cylindrical SU8 aperture, 21% of the bilayers failed during the first five aspiration cycles, whereas 79% of the bilayers were still intact after the first five cycles, but none of the bilayers survived 15 aspiration cycles. When eight bilayers were suspended in a beak-shaped aperture of 80 μm diameter, 62% of the bilayers withstood the first five aspiration cycles, whereas 38% of the bilayers survived up to 15 cycles (with all bilayers failing between 15 and 25 cycles), representing a marked improvement in bilayer stability.

Although the bilayer lifetime, in the absence of perturbation of the aqueous compartments, was comparable for triangle-shaped and beak-shaped apertures (see above), the mechanical stability of bilayers suspended in these two apertures is quite different. Remarkably, bilayers in the triangle-shaped apertures withstood up to 25 aspiration cycles in 70% of 10 independent experiments, up to 35 and 45 cycles in 60% and 40% of experiments, respectively, and even after 55 cycles one of the 10 bilayers was still intact. These data clearly illustrate that the mechanical stability of the DOPC/POPG folded bilayers is substantially enhanced by the triangle profile of the aperture walls.

Ion channel incorporation via vesicle fusion

To demonstrate their use for the characterization of macromolecular ion channel proteins, we employed proteoliposomes with the potassium channel KcsA from *Streptomyces lividans* to show bilayer recordings of an integral membrane protein. One of two aqueous compartments contained a buffer solution of pH 4.0 because KcsA is a pH-gated channel that does not display channel activity at neutral or alkaline pH (48,58–60).

Fig. 6, *B* and *C*, show channel activity in a POPG bilayer painted on a beak-shaped aperture with an inner diameter of 60 μm, and in a DOPC/POPG (1:1 molar ratio) bilayer painted on a larger, 80 μm diameter, beak-shaped aperture. These bilayer current steps are characteristic for KcsA gating and demonstrate that the KcsA has been incorporated into the suspended lipid bilayer by proteoliposome fusion (60). As seen in Fig. 6, at +150 mV, a burst of ion channel activity was obtained with amplitude of 27.4 $\pm$ 0.86 pA and opening probability of 0.63 for POPG bilayer, which correspond with the literature on KcsA gating (48,61). It is noteworthy that ion channel activity was never observed when the total capacitance was <40 pF, implying that bilayers that are smaller than ~60 μm in diameter did not support KcsA incorporation through proteoliposome fusion. Hence for proteoliposome delivery of ion channels, beak-shaped apertures with a diameter of 80 μm were preferred. Significantly smaller beak-shaped apertures with suspended bilayers did not consistently support KcsA gating, whereas significantly larger apertures did not result in stable suspended bilayers (see above). We also observed that bilayers painted from nonane rather than decane did not display KcsA current events, neither in 60 μm nor in 80 μm diameter beak-shaped apertures, indicating that nonane modulated the properties of the phospholipid bilayer (55,62). Furthermore, folded bilayers in shaped apertures supported ion channel activity of alamethicin and of proteoliposome-delivered pore domains of voltage-gated sodium and potassium channels (S. Kalsi, unpublished data).

DISCUSSION

Montal and Mueller used a 25-μm thick Teflon film as the septum in their original report on the folded bilayer method (10), and Teflon sheets have remained the material of choice for BLM electrophysiology with homemade apertures. Teflon is mechanically robust, allowing handling and clamping between bilayer chambers of thin sheets, chemically stable, sufficiently hydrophobic (~110° contact angle) to be wetted by annulus solvents such as decane, and its low dielectric constant of 2.1 implies that clamped Teflon sheets only contribute a small background capacitance, which is important for low-noise (high bandwidth) electrical measurements (16). Apertures in Teflon can be created by mechanical means such as punching with a hot wire or with an electrical spark discharge (19). However,

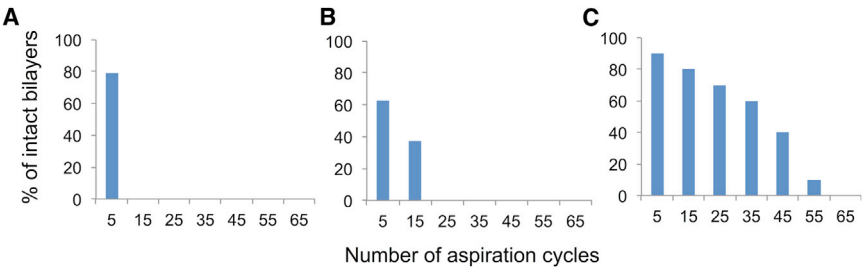

FIGURE 7 Stability of folded bilayers of DOPC/POPG (1:1 molar ratio) in various apertures, quantified as the number of aspiration cycles that can be withstood by the bilayer. (*a*) Cylindrical aperture of 80 μm diameter (n = 19), (*b*) beak-shaped aperture of 80 μm diameter (n = 8), (*c*) triangle-shaped aperture of 80 μm diameter (n = 10). To see this figure in color, go online.

lithography-based studies, aimed at reproducible aperture fabrication, have avoided the use of Teflon because its chemical inertness implies that it cannot be wet etched, complicating pattern transfer from an aperture-defining photoresist layer.

Instead, apertures have been fabricated in traditional microelectronics materials such as silicon and silicon nitride (26,31,34,45), and also directly in photoresist layers (23,27,41–43). Because the intrinsic capacitance of silicon and silicon composites is high, apertures in these materials can only be used for single-channel recordings if the capacitance is reduced by a (hydrophobic) coating of a material with a low dielectric constant, an approach that has been demonstrated recently by Niwano and co-workers for triangle-shaped apertures in silicon nitride (46,47). Apertures in photoresists, polyimide-based Pyralin and epoxy-based SU8, have also been shown to enable bilayer formation, despite their moderate hydrophobicity (~75° contact angle) (27,41–43), although a hydrophobic coating of SU8 has also been reported (23). Conveniently, the electrical and mechanical properties of these resists closely resemble those of Teflon. Another advantage of photosensitive materials, in the context of bilayer stabilization, is that a wide range of aperture shapes can be created by three-dimensional laser lithography, whereas aperture outlines in silicon-type materials are limited by (an)isotropic etching profiles.

In this study, we used shaped apertures in SU8 to investigate whether aperture-localized thinning of the septum stabilizes aperture-suspended bilayers. For both the painting and the folding method, bilayer lifetimes of >20 h were routinely obtained for triangle- and beak-shaped apertures with a tip thickness of ~2 μm and inner diameters of 60 or 80 μm, whereas 100 μm diameter tapered apertures resulted in the same limited bilayer lifetime (1–2 h) as nonshaped cylindrical SU8 apertures of 60 μm diameter. In combination with a control experiment with a beak-shaped aperture with a larger tip thickness of ~10 μm, which resulted in bilayer lifetimes of ~14 h, these experiments demonstrated that a reduced septum thickness enhances the stability of painted and folded bilayers when the aperture diameter is smaller than ~100 μm. Mechanical bilayer stability measurements with folded bilayers supported this conclusion, also showing that triangle-shaped apertures could withstand up to three times as many aspiration cycles as beak-shaped apertures, which indicates that the geometry of the aperture in the vicinity of the tip also has an influence on bilayer stability.

Although previous studies with tapered, triangle-shaped, apertures have not explored aperture diameter and shape variations (41–47) and, except for Oshima et al. and Hirano-Iwata et al. (45,46), have not addressed bilayer mechanical stability, they do report bilayer lifetimes of tens of hours, in full agreement with our data. However, it is not clear why tapered apertures result in drastically enhanced lifetimes and mechanical stability of suspended bilayers. Although a reduced mismatch between the thickness of a lipid bilayer and the height of the wall of the aperture has been cited for tapered (i.e., thin-edged) apertures, this argument does not seem to apply to our apertures, which have an edge height that is still 400-fold larger than the bilayer thickness. Moreover, bilayer stability is linked to annulus stability, which in turn relates to favorable contact angles of the solvent with the aperture material (14). Indeed, Beerlink et al. (15) recently obtained a cross-sectional view of the decane annulus of a suspended bilayer in a kapton (polyimide) channel by x-ray propagation imaging, which visualizes how the annulus connects the bilayer to the solid material by wetting tens of micrometers of the kapton channel wall. We speculate that the shaped apertures stabilize the bilayer by providing an anchor region for the annulus, with the shape and hydrophobicity of the tapered regions preventing excessive drainage or lateral movement of the solvent annulus.

Because rupturing of a bilayer is not a process occurring uniformly over the whole surface, but rather originates in one or more discreet regions from where it spreads (63), bilayers can be stabilized by reducing the aperture diameter while maintaining a cylindrical aperture geometry (63,64). A concern about smaller bilayers, however, is that they might not be suitable for recordings of non water-soluble ion channels. It has been suggested that bilayers with a diameter smaller than ~30 μm do not support proteoliposome fusion and hence integral ion channels such as KcsA cannot be incorporated into the bilayer (5,6,38,39), which may be due to unstirred layer effects in high aspect ratio apertures (65). However, we also noted this relation between bilayer size and ion channel activity with our triangle- and beak-shaped apertures in SU8. When the bilayer was considerably smaller than 60 μm (<40 pF capacitance) we never observed KcsA channel activity, and bilayers formed in 60 μm diameter apertures were usually, but not always, large enough, whereas bilayers formed in 80 μm variations readily resulted in KcsA channel activity. In our opinion, this highlights the need to verify novel bilayer stabilization strategies with proteoliposome-delivered channels rather than, exclusively, with robust channels such as the polypeptides gramicidin and alamethicin and the highly stable and water-soluble α-hemolysin, all of which can be delivered via the aqueous compartment.

In conclusion, the shaped apertures developed in this study provide stable high quality lipid bilayers that support ion channel activity of both self-incorporating and proteoliposome-delivered ion channels throughout the lifetime of the bilayer. The use of 50-μm thick Parylene-coated SU8 as a septum, thinned only at the aperture area, gives a low background capacitance of 18 pF, enabling high-bandwidth recordings, exemplified by the measured 1 pA peak-to-peak noise at 1 kHz filtering. These SU8 sheets are of sufficient strength to be clamped in vertical bilayer chambers and optically accessible horizontal chips. In our experience, the use of tapered apertures with reproducible geometries

substantially increases the throughput of single-channel BLM experiments by accelerating the bilayer formation process and minimizing bilayer failure during proteoliposome and drug addition. We note that the folding method is completely compatible with pipetting robots (66) and that bilayers, which are sufficiently stable to withstand multiple aspiration cycles, are suitable for the development of automated parallel BLM electrophysiology platforms, analogous to the advance of automated planar patch clamp instrumentation (2).

The authors gratefully acknowledge funding from the Engineering and Physical Sciences Research Council through grants EP/H044795/1 (to H.M. and M.dP.) and EP/H043888/1 (to B.A.W.).

REFERENCES

1. Hille, B. 2001. *In* Ion Channels of Excitable Membranes Sinauer Associates, Sunderland, MA, pp. 1–22.
2. Dunlop, J., M. Bowlby, …, R. Arias. 2008. High-throughput electrophysiology: an emerging paradigm for ion-channel screening and physiology. *Nat. Rev. Drug Discov.* 7:358–368.
3. Xu, J., X. Wang, …, J. Xu. 2001. Ion-channel assay technologies: quo vadis? *Drug Discov. Today.* 6:1278–1287.
4. Trapani, J. G., and S. J. Korn. 2003. Control of ion channel expression for patch clamp recordings using an inducible expression system in mammalian cell lines. *BMC Neurosci.* 4:15.
5. Demarche, S., K. Sugihara, …, J. Vörös. 2011. Techniques for recording reconstituted ion channels. *Analyst (Lond.).* 136:1077–1089.
6. Williams, A. J. 1994. An introduction to the methods available for ion channel reconstitution. *In* Microelectrode Techniques. D. C. Odgen, editor. The Company of Biologists, Cambridge, pp. 79–99.
7. Alvarez, O. 1986. How to set up a bilayer system. *In* Ion Channel Reconstitution. C. Miller, editor. Plenum Press, New York, pp. 115–130.
8. de Planque, M. R. R., G. P. Mendes, …, H. Morgan. 2006. Controlled delivery of membrane proteins to artificial lipid bilayers by nystatin-ergosterol modulated vesicle fusion. *IEE Proc., Nanobiotechnol.* 153:21–30.
9. Mueller, P., D. O. Rudin, …, W. C. Wescott. 1962. Reconstitution of cell membrane structure *in vitro* and its transformation into an excitable system. *Nature.* 194:979–980.
10. Montal, M., and P. Mueller. 1972. Formation of bimolecular membranes from lipid monolayers and a study of their electrical properties. *Proc. Natl. Acad. Sci. USA.* 69:3561–3566.
11. White, S. H., D. C. Petersen, …, M. Yafuso. 1976. Formation of planar bilayer membranes from lipid monolayers. A critique. *Biophys. J.* 16:481–489.
12. White, S. H. 1986. The physical nature of planar bilayer membranes. *In* Ion Channel Reconstitution. C. Miller, editor. Plenum Press, New York, pp. 3–35.
13. Pelzer, D. J., T. F. McDonald, and S. Pelzer. 1993. Reconstitution of muscle calcium channel function in bilayer membranes: from the first steps to results. *In* Methods in Pharmacology, *Vol. 7*. Glossmann, H., and J. Striessnig, editors. Plenum Press, New York, pp. 99–140.
14. White, S. H. 1972. Analysis of the torus surrounding planar lipid bilayer membranes. *Biophys. J.* 12:432–445.
15. Beerlink, A., S. Thutupalli, …, T. Salditt. 2012. X-ray propagation imaging of a lipid bilayer in solution. *Soft Matter.* 8:4595–4601.
16. Wonderlin, W. F., A. Finkel, and R. J. French. 1990. Optimizing planar lipid bilayer single-channel recordings for high resolution with rapid voltage steps. *Biophys. J.* 58:289–297.
17. Mayer, M., J. K. Kriebel, …, G. M. Whitesides. 2003. Microfabricated teflon membranes for low-noise recordings of ion channels in planar lipid bilayers. *Biophys. J.* 85:2684–2695.
18. O'Shaughnessy, T. J., J. E. Hu, …, F. S. Ligler. 2007. Laser ablation of micropores for formation of artificial planar lipid bilayers. *Biomed. Microdevices.* 9:863–868.
19. Maglia, G., A. J. Heron, …, H. Bayley. 2010. Analysis of single nucleic acid molecules with protein nanopores. *In* Methods in Enzymology. N. G. Walter, editor. Academic Press, Massachusetts, pp. 591–623.
20. Reimhult, E., and K. Kumar. 2008. Membrane biosensor platforms using nano- and microporous supports. *Trends Biotechnol.* 26:82–89.
21. Kumar, K., L. Isa, …, E. Reimhult. 2011. Formation of nanopore-spanning lipid bilayers through liposome fusion. *Langmuir.* 27:10920–10928.
22. Bally, M., K. Bailey, …, B. Städler. 2010. Liposome and lipid bilayer arrays towards biosensing applications. *Small.* 6:2481–2497.
23. Cheng, Y., R. J. Bushby, …, S. D. Ogier. 2001. Single ion channel sensitivity in suspended bilayers on micromachined supports. *Langmuir.* 17:1240–1242.
24. Peterman, M. C., J. M. Ziebarth, …, D. M. Bloom. 2002. Ion channels and lipid bilayer membranes under high potentials using microfabricated apertures. *Biomed. Microdevices.* 4:231–236.
25. Sondermann, M., M. George, …, J. C. Behrends. 2006. High-resolution electrophysiology on a chip: transient dynamics of alamethicin channel formation. *Biochim. Biophys. Acta.* 1758:545–551.
26. Simon, A., A. Girard-Egrot, …, A. Fuchs. 2007. Formation and stability of a suspended biomimetic lipid bilayer on silicon submicrometer-sized pores. *J. Colloid Interface Sci.* 308:337–343.
27. Baaken, G., M. Sondermann, …, J. C. Behrends. 2008. Planar microelectrode-cavity array for high-resolution and parallel electrical recording of membrane ionic currents. *Lab Chip.* 8:938–944.
28. Kocun, M., T. D. Lazzara, …, A. Janshoff. 2011. Preparation of solvent-free, pore-spanning lipid bilayers: modeling the low tension of plasma membranes. *Langmuir.* 27:7672–7680.
29. Buchholz, K., A. Tinazli, …, M. Tornow. 2008. Silicon-on-insulator based nanopore cavity arrays for lipid membrane investigation. *Nanotechnology.* 19:445305.
30. Fertig, N., C. Meyer, …, J. C. Behrends. 2001. Microstructured glass chip for ion-channel electrophysiology. *Phys. Rev. E Stat. Nonlin. Soft Matter Phys.* 64:040901.
31. Wilk, S. J., M. Goryll, …, R. S. Eisenberg. 2004. Teflon-coated silicon apertures for supported lipid bilayer membranes. *Appl. Phys. Lett.* 85:3307–3309.
32. Han, X., A. Studer, …, L. X. Tiefenauer. 2007. Nanopore arrays for stable and functional free-standing lipid bilayers. *Adv. Mater.* 19:4466–4470.
33. Kitta, M., H. Tanaka, and T. Kawai. 2009. Rapid fabrication of Teflon micropores for artificial lipid bilayer formation. *Biosens. Bioelectron.* 25:931–934.
34. Goryll, M., and N. Chaplot. 2009. Miniaturized silicon apertures for lipid bilayer reconstitution experiments. *MRS Proceedings.* 1191:79–86.
35. Gu, L.-Q., and J. W. Shim. 2010. Single molecule sensing by nanopores and nanopore devices. *Analyst (Lond.).* 135:441–451.
36. Kawano, R., T. Osaki, and S. Takeuchi. 2010. A parylene nanopore for stable planar lipid bilayer membranes. *Proc. IEEE Micro Electro Mechanical Systems (MEMS).* 23:923–926.
37. Korman, C. E., M. Megens, …, D. A. Horsley. 2013. Nanopore-spanning lipid bilayers on silicon nitride membranes that seal and selectively transport ions. *Langmuir.* 29:4421–4425.
38. Studer, A., S. Demarche, …, L. Tiefenauer. 2011. Integration and recording of a reconstituted voltage-gated sodium channel in planar lipid bilayers. *Biosens. Bioelectron.* 26:1924–1928.
39. Introduction to the BLM workstation. http://www.warneronline.com/product_info. Accessed March 15, 2013.

40. Niles, W. D., and F. S. Cohen. 1987. Video fluorescence microscopy studies of phospholipid vesicle fusion with a planar phospholipid membrane. Nature of membrane-membrane interactions and detection of release of contents. *J. Gen. Physiol.* 90:703–735.

41. Eray, M., N. S. Dogan, …, B. J. Van Wie. 1994. Highly stable bilayer lipid membranes (BLMs) formed on microfabricated polyimide apertures. *Biosens. Bioelectron.* 9:343–351.

42. Eray, M., N. S. Dogan, …, W. C. Davis. 1995. A highly stable and selective biosensor using modified nicotinic acetylcholine receptor (nAChR). *Biosystems.* 35:183–188.

43. Liu, B., D. Rieck, …, D. A. Kidwell. 2009. Bilayer lipid membrane (BLM) based ion selective electrodes at the meso-, micro-, and nanoscales. *Biosens. Bioelectron.* 24:1843–1849.

44. Hirano-Iwata, A., A. Oshima, …, M. Niwano. 2010. Stable lipid bilayers based on micro- and nano-fabrication. *Supramol. Chem.* 22:406–412.

45. Hirano-Iwata, A., K. Aoto, …, M. Niwano. 2010. Free-standing lipid bilayers in silicon chips-membrane stabilization based on microfabricated apertures with a nanometer-scale smoothness. *Langmuir.* 26:1949–1952.

46. Oshima, A., A. Hirano-Iwata, …, M. Niwano. 2012. Mechanically stable lipid bilayers in Teflon-coated silicon chips for single-channel recordings. *Micro and Nanosystems.* 4:2–7.

47. Oshima, A., A. Hirano-Iwata, …, M. Niwano. 2013. Reconstitution of human ether-a-go-go-related gene channels in microfabricated silicon chips. *Anal. Chem.* 85:4363–4369.

48. Marius, P., M. Zagnoni, …, A. G. Lee. 2008. Binding of anionic lipids to at least three nonannular sites on the potassium channel KcsA is required for channel opening. *Biophys. J.* 94:1689–1698.

49. Sandison, M. E., M. Zagnoni, and H. Morgan. 2007. Air-exposure technique for the formation of artificial lipid bilayers in microsystems. *Langmuir.* 23:8277–8284.

50. Marie, R., S. Schmid, …, M. Dufva. 2006. Immobilization of DNA to polymerized SU-8 photoresist. *Biosens. Bioelectron.* 21:1327–1332.

51. Sikanen, T., L. Heikkilä, …, T. Kotiaho. 2007. Performance of SU-8 microchips as separation devices and comparison with glass microchips. *Anal. Chem.* 79:6255–6263.

52. Antonov, V. F., E. V. Shevchenko, …, A. V. Frolov. 1992. Stable cupola-shaped bilayer lipid membranes with mobile Plateau-Gibbs border: expansion-shrinkage of membrane due to thermal transitions. *Chem. Phys. Lipids.* 61:219–224.

53. Cassiday, L. 2007. A portable protein nanopore. *Anal. Chem.* 79:3979.

54. Costa, J. A., D. A. Nguyen, …, B. Hanss. 2013. Wicking: a rapid method for manually inserting ion channels into planar lipid bilayers. *PLoS ONE.* 8:e60836.

55. McIntosh, T. J., S. A. Simon, and R. C. MacDonald. 1980. The organization of *n*-alkanes in lipid bilayers. *Biochim. Biophys. Acta.* 597:445–463.

56. Akabas, M. H., F. S. Cohen, and A. Finkelstein. 1984. Separation of the osmotically driven fusion event from vesicle-planar membrane attachment in a model system for exocytosis. *J. Cell Biol.* 98:1063–1071.

57. Cohen, F. S. 1986. Fusion of liposomes to planar bilayers. *In* Ion Channel Reconstitution. C. Miller, editor. Plenum Press, New York, pp. 131–139.

58. Seeger, H. M., L. Aldrovandi, …, P. Facci. 2010. Changes in single K^+ channel behavior induced by a lipid phase transition. *Biophys. J.* 99:3675–3683.

59. McCoy, J. G., and C. M. Nimigean. 2012. Structural correlates of selectivity and inactivation in potassium channels. *Biochim. Biophys. Acta.* 1818:272–285.

60. LeMasurier, M., L. Heginbotham, and C. Miller. 2001. KcsA: it's a potassium channel. *J. Gen. Physiol.* 118:303–314.

61. Chakrapani, S., J. F. Cordero-Morales, and E. Perozo. 2007. A quantitative description of KcsA gating II: single-channel currents. *J. Gen. Physiol.* 130:479–496.

62. Fettiplace, R., D. M. Andrews, and D. A. Haydon. 1971. The thickness, composition and structure of some lipid bilayers and natural membranes. *J. Membr. Biol.* 5:277–296.

63. Ti Tien, H. 1968. Black lipid membranes at bifaces : formation characteristics, optical and some thermodynamic properties. *J. Gen. Physiol.* 52:125–144.

64. Andersen, O. S. 1983. Ion movement through gramicidin A channels. Single-channel measurements at very high potentials. *Biophys. J.* 41:119–133.

65. Zhu, Z. W., Y. Wang, …, B. W. Mao. 2012. Electrochemical impedance spectroscopy and atomic force microscopic studies of electrical and mechanical properties of nano-black lipid membranes and size dependence. *Langmuir.* 28:14739–14746.

66. Rossi, M., F. Thei, and M. Tartagani. 2012. A parallel sensing technique for automatic bilayer lipid membrane arrays monitoring. *Sensors Transducers J.* 14:185–196.